

Boosting Safe Human-Robot Collaboration Through Adaptive Collision Sensitivity

Lukas Rustler*, Matej Misar*, and Matej Hoffmann

Abstract—What is considered safe for a robot operator during physical human-robot collaboration (HRC) is specified in corresponding HRC standards (e.g., the European ISO/TS 15066). The regime that allows collisions between the moving robot and the operator, called Power and Force Limiting (PFL), restricts the permissible contact forces. Using the same fixed contact thresholds on the entire robot surface results in significant and unnecessary productivity losses, as the robot needs to stop even when impact forces are within limits. Here we present a framework for setting the protective skin thresholds individually for different parts of the robot body and dynamically on the fly, based on the effective mass of each robot link and the link velocity. We perform experiments on a 6-axis collaborative robot arm (UR10e) completely covered with a sensitive skin (AIRSKIN) consisting of eleven individual pads. On a mock pick-and-place scenario with both transient and quasi-static collisions, we demonstrate how skin sensitivity influences the task performance and exerted force. We show an increase in productivity of almost 50% from the most conservative setting of collision thresholds to the most adaptive setting, while ensuring safety for human operators. The method is applicable to any robot for which the effective mass can be calculated.

I. INTRODUCTION

Robots are leaving safety fences and start to share workspace or even living space with humans. As they leave controlled environments and enter domains that are much less structured, they need to dynamically adapt to unpredictable interactions and guarantee safety at every moment. There has been rapid development in this field of physical human-robot interaction (pHRI) or human-robot collaboration (HRC) in the last decade (see [1]–[3] for surveys), a growing market of collaborative robots, along with the introduction and revision of new safety standards ([4]–[6]). According to [6], there are two main ways of satisfying the safety requirements when a human physically collaborates with a robot: (i) Power and Force Limiting (PFL) and (ii) Speed and Separation Monitoring (SSM). For PFL, physical contacts with a moving robot are allowed, but the forces, pressures, and energy absorbed during a collision need to be within part-specific limits of the human body. This translates into lightweight structure, soft padding,

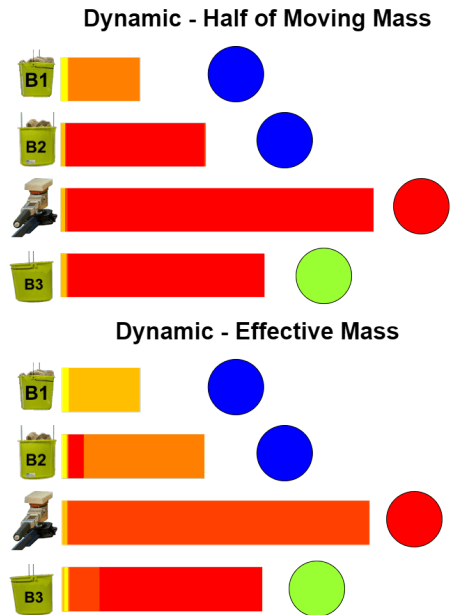
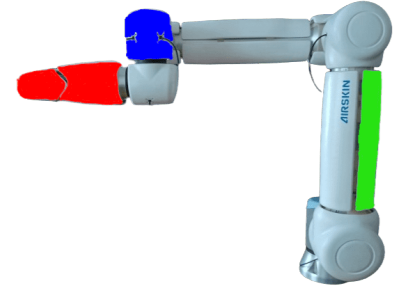


Fig. 1: The robot used with AIRSKIN. (Top) The colored skin parts are used for collisions in our experiments—the colors are used just for illustration and to relate given skin links to given collision places. (Bottom) The colored bars represent the dynamically set sensitivity thresholds when the different robot links collide with a specific obstacle (blue circles indicate the the blue robot link collides with B1 and B2). The thresholds range from most sensitive (red) to the least sensitive (yellow). See Section IV for more details.

*Both authors contributed equally.

Lukas Rustler, Matej Misar, and Matej Hoffmann are with the Department of Cybernetics, Faculty of Electrical Engineering, Czech Technical University in Prague, lukas.rustler@fel.cvut.cz, matej.hoffmann@fel.cvut.cz.

This work was co-funded by the European Union under the project Robotics and Advanced Industrial Production (reg. no. CZ.02.01.01/00/22_008/0004590). L.R. was additionally supported by the Grant Agency of the Czech Technical University in Prague, grant No. SGS24/096/OHK3/2T/13. We thank Bedrich Himmel for assistance with the construction of the setup

and no pinch points on the robot side, in combination with robot interaction control methods for the post-impact phase: collision detection and response relying on motor load measurements, force/torque, or joint torque sensing (e.g., [7]). However, the speed and payload of robots that comply with this safety requirement is limited.

Furthermore, in practice, exploiting the full potential of the PFL regime, i.e., stopping the robot only if the prescribed

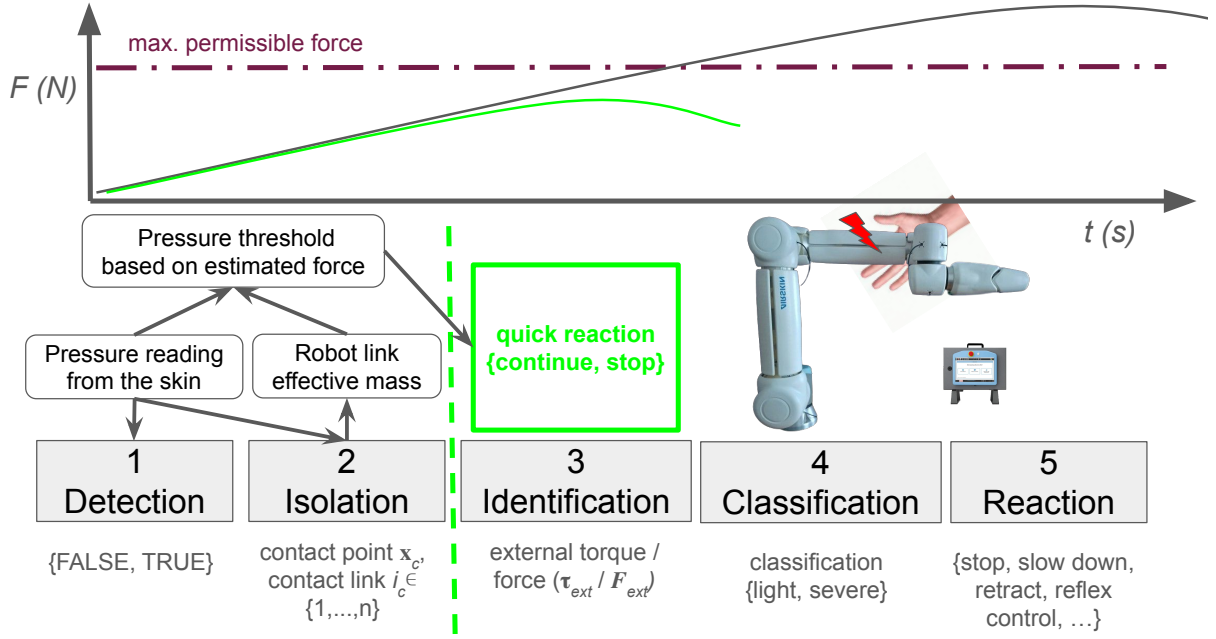


Fig. 2: Schematic overview. Collision handling pipeline in the bottom part adapted from [8]. See text for details.

force threshold is exceeded, is difficult or impossible. According to [8], a collision needs to be 1) detected, 2) isolated (which robot link and which location on the link), 3) identified (estimating the external torque or force), 4) classified, and 5) then a robot reaction is triggered – see the bottom part of Fig. 2. The accuracy or even the possibility of performing some of these steps depends on the type of contact (single or multiple), the contact location, and in particular on the sensory equipment of the robot. Electronic skins covering large parts of the robot surface [9]–[12] facilitate detection and isolation. For identification, force/torque or joint torque sensors together with accurate models of the robot dynamics are the best. However, correct estimation of forces, pressures, and energies on the body of the human operator is not possible for several reasons. First, only the first very brief evolution of the collision is used for collision identification. According to PFL, the first 0.5s should be considered for transient contact and even longer for quasi-static contact. Second, even if external force on the robot body can be estimated, applying Newton’s third law and assuming that the same force acts on the human body is problematic. Third, without additional visual sensors, the robot does not know with which part of the body it is colliding (different limits apply and different tissue stiffness is needed to model the collision). In practice, collaborative robot applications are thus configured too conservatively, i.e. stopping the robot as soon as a collision is detected. Frequent stops of the robot then negatively impact productivity.

In this work, we present a new method that aims to maximize productivity in the PFL regime as illustrated in Fig. 2. The main idea is to perform only collision detection and isolation, which are relatively easy and can be performed

fast, and trigger a robot reaction—if necessary. The collision is detected and isolated using a pressure-sensitive electronic skin (AIRSKIN) covering the entire robot body. The key innovation here is that we online estimate the collision force from the robot velocity and effective mass¹ and then use that estimate to set a threshold to compare with the pressure value measured by the protective skin. If the estimated force is low, the robot will react by continuing the execution of the task.

To our knowledge, this is the first study that adaptively sets collision thresholds on a collaborative robot that brings safety (force limits according to [6]) and productivity under one hood. Solutions for use in industry such as AIRSKIN normally employ the same threshold in all skin pads and use a highly sensitive setting, resulting in too frequent task interruptions. In research articles employing large-area skins, same thresholds are also typically employed (e.g., [14]).

Our recent work on this topic [15] introduced this idea, but was largely based on simulation and featured only preliminary real robot experiments. Here, we present systematic experiments on a real robot by utilizing a robust environment allowing for repeatable measurements. In addition, the skin thresholds have been redesigned (5 thresholds compared to 3 in [15] with a better selection of these thresholds) and more repetitions. The new experimental evaluation newly contains not only transient but also quasi-static (clamping) contacts.

¹Based on the simple formula from [6] extended by the more accurate effective mass calculation involving the position in the workspace and the collision direction [13].

II. METHOD

The core of this work is the evaluation of real-world impacts in a setup that simulated human-robot cooperation with several obstacles during a task performed by the robot. This section describes the theoretical background, setup, robot, and skin used during the experiments.

A. Robot, Skin and Software

The robot used in this work is a 6-Degree of Freedom (DoF) robotic manipulator UR10e. The arm itself is designed for collaborative purposes. Our robot is further equipped with robotic skin AIRSKIN². The skin is essential for our experiments. We are able to read the pressure values (in Pascals) from individual skin parts (also called pads; 11 of them placed on our robot) at approximately 30 Hz.

Both the robot and the skin are integrated and interconnected using Robot Operating System (ROS) middleware. During the task performed by the robot (see next Section), we utilize control in joint velocity space to allow for quick reactions to impacts.

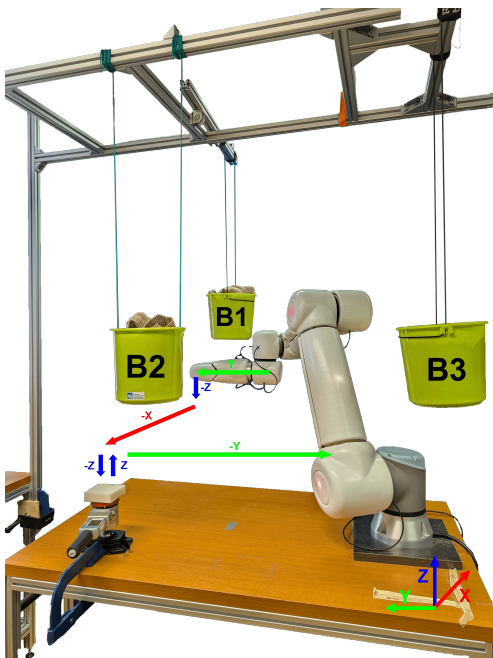


Fig. 3: The environment used for the experiments. The buckets hung on a rope simulate transient contacts, and the measuring device fixed on a table simulates the quasi-static clamping scenario.

B. Task and Environment

The environment (Fig. 3) we developed to perform the experiments consists of three buckets (B1, B2, B3) hung on a rope from the ceiling. The buckets are filled with small stones with a total weight of 5.6 kg. The weight was selected according to the average weight of the whole human arm from ISO/TS 15066 [6]. The buckets can freely move in

the space, thus simulating the impact of the robot with the human arm. The impacts with buckets are transient, that is, dynamic impacts in which a human body part is impacted by a moving robot and the human can recoil or retract [6]. The setup also includes *CBSF-75-Basic* certified measuring device for validation of collaborative tasks with the range of 20 N to 500 N. This device is firmly attached to the table and is used to simulate a clamping scenario. This impact is quasi-static, that is, impact of a human body part with the robot, when the robot clamps or crushes the human for a prolonged period of time [6].

To be able to evaluate the effect of different collision threshold settings on performance, we define a mock pick-and-place task – see the accompanying video. The direction of the movements is depicted in Fig. 3. The order of movements starts from the top green line (movement in the y-axis of the robot) and collision with the first bucket B1, continues with slight downward movement (negative z-axis) and movement in the robot's x-axis. Then it continues with impact to B2. The robot then goes again downward to collide with the measuring device, and returns up after the collision. Finally, the robot moves in its negative y-axis and collides with bucket B3.

III. SKIN SENSITIVITY THRESHOLDS

The initial step in the pipeline is to select the individual sensitivity thresholds of our robotic skin. We decided to select five different sensitivity thresholds, numbered from 0 (the most sensitive one) to 4 (the least sensitive). The thresholds are represented as a percentage value of the pressure range in our application and were set individually for individual pads on the robot. We measured the pressure range for each pad by hitting obstacles. Then, we selected the most sensitive threshold to be robust (a low number of false negative detections), while being sensitive enough to perceive even gentle contact. The other thresholds are set as 25, 75, 95, and 110% of the pressure range. The reason we also selected 110% is to count for the cases when a collision is outside the distribution of the ranges we measured (which is in theory possible, as we measured each range only five times).

IV. THRESHOLD SETTING STRATEGIES

The core components are the strategies to set sensitivity thresholds for individual skin parts. We can divide our strategies to two main sections: (i) uniform (static) distribution of sensitivity thresholds; (ii) dynamic distribution.

The first option is straightforward. We set all the pads on the robot to the same (uniform) sensitivity thresholds. As we have five different thresholds, we tested five different static settings based on the threshold—*Uniform 0*, *Uniform 1*, *Uniform 2*, *Uniform 3*, *Uniform 4*.

The dynamic setting is more complicated and is divided into two methods.

²<https://www.airskin.io/>

1) *Dynamic – Half of Moving Mass (HMM)*: The first method is based purely on equation from ISO/TS 15066 [6], that defines the maximal allowed velocity given permissible force limit as

$$v \leq \frac{F_{\max}}{\sqrt{k}} \sqrt{m_R^{-1} + m_H^{-1}}, \quad (1)$$

where k is the spring constant of impacted human body, m_R is the effective mass of the robot, m_H is the effective mass of the impacted human body, v is the Cartesian velocity of the robot link and F_{\max} is the maximal permissible force. The force F_{\max} can be computed as

$$F_{\max} = \frac{v\sqrt{k}}{\sqrt{m_R^{-1} + m_H^{-1}}}. \quad (2)$$

The spring constant k is fixed in our experiments to 75 000 N/m corresponding to the spring constant of the back of the non-dominant hand as suggested by ISO/TS 15066. We selected the mass m_H as 5.6 kg (and we made our buckets weigh the same) based on the average weight of human arm defined also in [6]. The mass m_R is in ISO/TS 15066 defined as Half of Moving Mass (HMM) of the robot. In our experiments, this weight is computed half of the mass of the sum of weights of links up to the link with skin part in collision. This mass is the main difference from the second dynamic policy.

2) *Dynamic – Effective Mass (EM)*: This policy also uses Eq. 2 to compute the permissible force. However, now m_R is actually the Effective Mass (EF) of the robot. EF is a property of the robot (each point of the robot), which can be computed using the dynamics of the robot [13]. The EF is always computed in a given direction. We consider this direction to be the direction of the link on which is the skin pad that detected collision. Using this direction \mathbf{u} , one can compute the effective mass $m_{\mathbf{u}}$ as

$$m_{\mathbf{u}} = \frac{1}{\mathbf{u}^T \mathbf{\Lambda}_v(\mathbf{q})^{-1} \mathbf{u}}, \quad (3)$$

where $\mathbf{\Lambda}_v(\mathbf{q})^{-1}$ is the upper 3×3 matrix of Cartesian kinetic energy matrix $\mathbf{\Lambda}(\mathbf{q})^{-1}$, that can be computed as

$$\mathbf{\Lambda}(\mathbf{q})^{-1} = \mathbf{J}(\mathbf{q})\mathbf{M}(\mathbf{q})\mathbf{J}(\mathbf{q})^T, \quad (4)$$

where $\mathbf{M}(\mathbf{q})$ is the joint space inertia matrix.

This property of robots is well known in the community, but is arguably still not used often. The reason is its sensitivity to proper dynamic model of the robot and instability in some configurations (mainly near the base of the robot; see [16] for discussion on the topic). We provide some examples in Fig. 4, where the EF in every configuration of our task is shown for three skin pads (the pads are in collision with any of the obstacles). We can see that the EF is in most cases lower than HMM, which was our motivation to use this property in our dynamic threshold setting policy. However, we can also see that it is higher in the beginning of the task for one of the pads. The given skin part (green pad in Fig. 1) is in the beginning of the movement very close to the robot base and is moving in such a way that it realistically

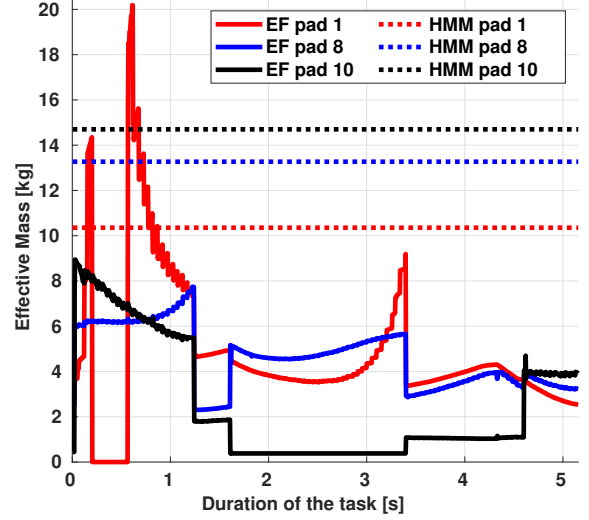


Fig. 4: Effective Mass (EF) and Half of Moving Mass (HMM) for three skin parts in every configuration of the performed task.

cannot exert any force to obstacles (see the attached video). Although it is important to keep this in mind, we still believe that the utilization of EF could have a high impact not only on Human-Robot Interaction (HRI) research.

Both of the dynamic methods have the same concept of setting of thresholds based on the estimated force. We set the thresholds from force by discretizing the possible force into five intervals. The intervals are different for transient and quasi-static contacts, as based on [6] the limits for permissible force are not the same—140 N and 280 N for quasi-static and transient contacts, respectively. Thus based on these limits, we set the five threshold from forces as

$$T_{\text{transient}} = \begin{cases} 0, & \text{if } F \geq 280 \text{ N} \\ 1, & \text{if } 200 \text{ N} \leq F < 280 \text{ N} \\ 2, & \text{if } 120 \text{ N} \leq F < 200 \text{ N} \\ 3, & \text{if } 40 \text{ N} \leq F < 120 \text{ N} \\ 4, & \text{if } F < 40 \text{ N}, \end{cases} \quad (5)$$

for transient contacts and

$$T_{\text{quasi-static}} = \begin{cases} 0, & \text{if } F \geq 140 \text{ N} \\ 1, & \text{if } 100 \text{ N} \leq F < 140 \text{ N} \\ 2, & \text{if } 60 \text{ N} \leq F < 100 \text{ N} \\ 3, & \text{if } 20 \text{ N} \leq F < 60 \text{ N} \\ 4, & \text{if } F < 20 \text{ N}, \end{cases} \quad (6)$$

for quasi-static contacts.

V. EXPERIMENTS AND RESULTS

This Section describes the experiments done. We performed several real-world experiments using our setup that mimics possible collision scenarios in human-robot cooperation scenario. All data collected during our experiment are available at <https://osf.io/9sq3t/>.

A. Experiments Settings

As stated in Section II-B, the robot performed a task inside our controlled environment with three buckets (5.6 kg each) that acted as obstacles (simulation of a collision with the human arm). For these obstacles, the robot was controlled to stop immediately after colliding with the robot skin at the moment a collision was detected. Consequently, the robot remains stopped for 1 s. If there is no longer a collision after the waiting period, the robot continues its task. If a new collision occurs at the same place (usually the bucket swings back to the robot), the robot stops again. After several collision detections (the number depends on skin sensitivity), the robot moves to the next location of its task. On top of the buckets, there is a measuring device located on the table, which simulates a clamping scenario between the robot and human operator. In case of a collision with this device, the robot is stopped again for 1 s, but now the robot moves back to the beginning of the current phase and then continues to the next waypoint of the task. The reason is that the measuring device cannot move out of the way of the robot, and thus the robot would stay in collision indefinitely.

The robot was controlled in joint velocity move so that the end-effector moves 600 mm s^{-1} . However, we had to make the movement towards the quasi-static collision half the speed (300 mm s^{-1}), because otherwise the internal safety controller of the robot always acted sooner than our robotic skin-enabled controller. We tested 7 different threshold settings and repeated each one of them five times, resulting in 35 total runs of the task (with more than 65 collisions among all the runs).

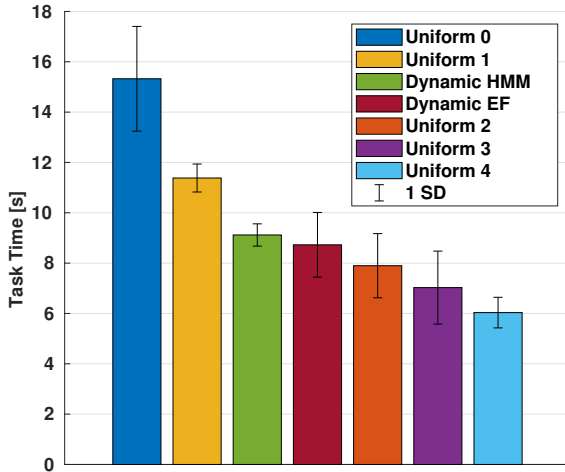


Fig. 5: Total task time for different thresholds settings. Each bar is average from 5 repetitions. Dynamic strategies uses Half of Moving Mass (HMM) and Effective Mass (EF).

B. Task Performance

The first and, arguably, the most straightforward metric to evaluate the effect of skin sensitivity and the sensitivity

setting method is the total time needed to complete the task. The results are shown in Fig. 5. We can see that, as expected, the more sensitive the skin, the longer the time required to complete the task. The difference between the most sensitive setting (*Uniform 0*) and the least sensitive one (*Uniform 4*) is, in average, more than 9 s, which is more than 200 % speed up.

The biggest reason for the difference in time between the uniform skin sensitivity settings is given by the number of collisions detected during the task. We provide a view on this parameter in Fig. 6. The first thing to notice is the total number of touches (detected collisions) for each sensitivity setting. The difference between *Uniform 0* and *Uniform 4* is, on average, more than 12 detections, which is a significant number. More specifically, the highest discrepancy in collision in different phases of the task is visible for collisions with buckets B1 and B3. For B3, the total number of collisions is low even in the most sensitive setting (*Uniform 0*), but is zero for *Uniform 2*, *Uniform 3*, and *Uniform 4*. For the case of bucket B1, the collision frequency starts at more than 8 collisions for *Uniform 0*, but drops to less than one for *Uniform 4*, showing the effect of skin sensitivity.

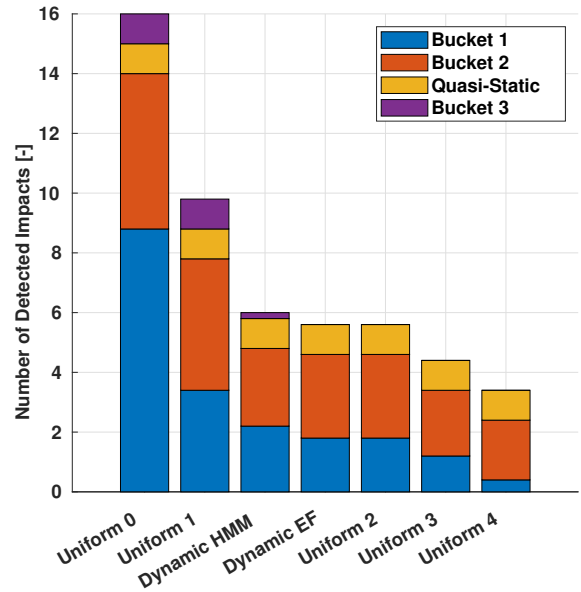


Fig. 6: Average detected collisions during the task for different thresholds settings. Each bar is averaged from 5 repetitions. Dynamic strategies uses Half of Moving Mass (HMM) and Effective Mass (EF).

So far, we have talked about uniform (static) settings of skin sensitivity on robotic skin. However, a more interesting and promising method for setting skin thresholds is the dynamic change of thresholds for individual skin parts based on Eq. 2. We tested two methods. One that directly uses the force estimation equation from ISO/TS 15066 [6] and one that also utilizes the so-called Effective Mass (EF) of the robot (see Section IV). We can again use Fig. 5 and Fig. 6. In

both of these, the two dynamic policies lie between *Uniform 1* and *Uniform 2*, while the effective mass version is slightly more efficient (both in terms of shorter total time and lower number of collisions with the obstacles).

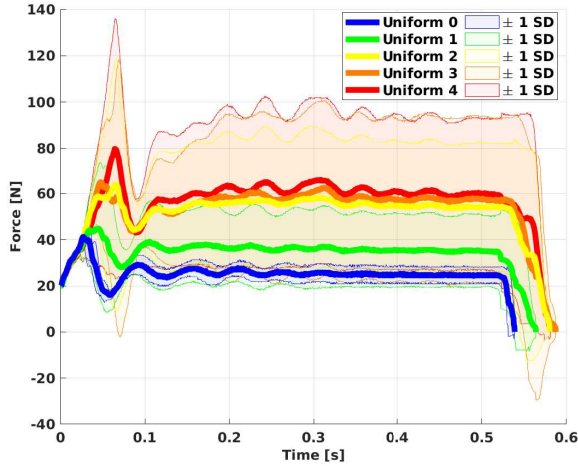


Fig. 7: Forces for different uniform thresholds (0 = most sensitive, . . . , 4 = least sensitive) with ± 1 Standard Deviation (SD).

It may seem that adaptive policies are worse than some of the uniform ones. However, it is necessary to take into account the safety and forces exerted by the robot using different skin sensitivity. Unfortunately, our force measuring device is not suitable to measure transient collisions, and thus we can confidently assess safety only using quasi-static collisions. In Fig. 7 we show averaged (over 5 repetitions) force evolutions measured during movement in the negative z-axis of the robot. We can see that the more sensitive the threshold, the lower the mean maximal force and the smaller the SD between individual repetitions. The same is shown in Table I, together with the forces measured during experiments with dynamic strategies. We also provide estimates from both dynamic policies that are used to select the sensitivity threshold.

	Force [N] ± 1 SD
<i>Uniform 0</i>	45.5 \pm 4.93
<i>Uniform 1</i>	59.6 \pm 20.4
<i>Uniform 2</i>	84.6 \pm 36.5
<i>Uniform 3</i>	87.6 \pm 44.6
<i>Uniform 4</i>	93.6 \pm 44.8
<i>Dynamic HMM (measured)</i>	54.0 \pm 26.1
<i>Dynamic EF (measured)</i>	61.8 \pm 27.8
<i>Dynamic HMM (estimated)</i>	166.5 \pm 1.67
<i>Dynamic EF (estimated)</i>	78.0 \pm 0.86

TABLE I: Real forces measured for quasi-static obstacle in every threshold setting and force estimates for dynamic policies. Dynamic strategies uses Half of Moving Mass (HMM) and Effective Mass (EF).

There are multiple things to reason about. First, we can see that the threshold sensitivity influences the exerted force

(both in amplitude and variance). Then, the dynamic policies both overestimate the real forces, but the superiority of using *Dynamic EF* is easily notable. The policy that uses directly the equation for force from ISO/TS 15066 estimates the force as 166 N, which is actually even over the official limit for quasi-static contacts (140 N). Thus, it sets the most sensitive threshold (see also Table II) which results in low real force (54 N). On the other hand, the policy that uses EF of the robot estimates the force as 78 N (less than half compared to the first dynamic method). That results in using the third most sensitive threshold (see again Table II) with real force measured of 61.8 N, which is considerably closer to the estimate. We can also look in Table II where the thresholds set by the dynamic methods for all collision places are shown. We can see that *Dynamic HMM* method sets the most sensitive thresholds everywhere, except for bucket B3. In contrast, the *Dynamic EF* sets the most sensitive threshold only for the first bucket and uses different thresholds for other obstacles.

	Impact Position [-]			
	B1	B2	QS	B3
<i>Dynamic HMM</i>	0	0	0	2
<i>Dynamic EF</i>	0	1	2	3

TABLE II: Thresholds (0 = most sensitive, . . . , 4 = least sensitive) selected for our two dynamic thresholds settings strategies for the three transient impacts (buckets B1, B2, B3) and quasi-static impact (QS). Dynamic strategies uses Half of Moving Mass (HMM) and Effective Mass (EF).

VI. CONCLUSION, DISCUSSION, AND FUTURE WORK

We introduced different strategies to set skin sensitivity thresholds—five uniform and two dynamic. We tested the policies in the real world with our custom environment that enabled us to simulate both transient and quasi-static collisions in a HRI task. We measured the impact forces in a quasi-static (clamping) scenario using a certified measuring device. We showed that skin sensitivity has an influence on task execution time, the number of collision detections, and the forces exerted. We further demonstrate that using a dynamic setting while computing Effective Mass (EF) of the robot can estimate the exerted force more precisely than using a basic formula from the corresponding ISO standard [6], providing better task performance while preserving human safety.

In this work, only the simplest reaction to a collision that exceeds a pressure threshold was applied: stop the robot. Post-collision reactions can have several forms and may also depend on what information is available about the collision (see collision identification in [8]) and on the robot capabilities (e.g., whether torque control is available [7]). In the setup used here—with coarse isolation of the collision location in space, a pressure value reading, and a velocity control mode—one possibility is to implement an avoidance reflex that will move the colliding robot link in the opposite direction (see [15]). Artificial skins with higher spatial resolution make it possible to move away the collision point along the normal to the robot skin at that location [17].

REFERENCES

- [1] S. Haddadin and E. Croft, "Physical Human-Robot Interaction," in *Springer Handbook of Robotics*. Springer, 2016, pp. 1835–1874.
- [2] W. Li, Y. Hu, Y. Zhou, and D. T. Pham, "Safe human–robot collaboration for industrial settings: A survey," *Journal of Intelligent Manufacturing*, vol. 35, no. 5, pp. 2235–2261, 2024.
- [3] V. Villani, F. Pini, F. Leali, and C. Secchi, "Survey on human–robot collaboration in industrial settings: Safety, intuitive interfaces and applications," *Mechatronics*, vol. 55, pp. 248–266, 2018.
- [4] "ISO 10218 Robots and robotic devices – Safety requirements for industrial robots – Part 1: Robots," International Organization for Standardization, Geneva, CH, Standard, 2011.
- [5] "ISO 10218 Robots and robotic devices – Safety requirements for industrial robots - Part 2: Robot systems and integration," International Organization for Standardization, Geneva, CH, Standard, 2011.
- [6] "ISO/TS 15066 Robots and robotic devices – Collaborative robots," International Organization for Standardization, Geneva, CH, Standard, 2016.
- [7] S. Haddadin, A. Albu-Schaffer, A. De Luca, and G. Hirzinger, "Collision Detection and Reaction: A Contribution to Safe Physical Human-Robot Interaction," in *2008 IEEE/RSJ International Conference on Intelligent Robots and Systems*, 2008, pp. 3356–3363.
- [8] S. Haddadin, A. De Luca, and A. Albu-Schäffer, "Robot collisions: A survey on detection, isolation, and identification," *IEEE Transactions on Robotics*, vol. 33, no. 6, pp. 1292 – 1312, 2017.
- [9] G. Cannata, M. Maggiali, G. Metta, and G. Sandini, "An Embedded Artificial Skin for Humanoid Robots," in *2008 IEEE International Conference on Multisensor Fusion and Integration for Intelligent Systems*. IEEE, 2008, pp. 434–438.
- [10] A. Goncalves, N. Kuppuswamy, A. Beaulieu, A. Uttamchandani, K. M. Tsui, and A. Alspach, "Punyo-1: Soft tactile-sensing upper-body robot for large object manipulation and physical human interaction," in *2022 IEEE 5th International Conference on Soft Robotics (RoboSoft)*. IEEE, 2022, pp. 844–851.
- [11] G. Cheng, E. Dean-Leon, F. Bergner, J. Rogelio Guadarrama Olvera, Q. Leboutet, and P. Mittendorfer, "A Comprehensive Realization of Robot Skin: Sensors, Sensing, Control, and Applications," *Proceedings of the IEEE*, vol. 107, no. 10, pp. 2034–2051, 2019.
- [12] P. Svarny, J. Rozlivek, L. Rustler, M. Sramek, Ö. Deli, M. Zillich, and M. Hoffmann, "Effect of Active and Passive Protective Soft Skins on Collision Forces in Human–Robot Collaboration," *Robotics and Computer-Integrated Manufacturing*, vol. 78, p. 102363, Dec. 2022.
- [13] O. Khatib, "Inertial Properties in Robotic Manipulation: An Object-Level Framework," *The International Journal of Robotics Research*, vol. 14, no. 1, pp. 19–36, 1995.
- [14] J. R. Guadarrama-Olvera, E. Dean-Leon, F. Bergner, and G. Cheng, "Pressure-Driven Body Compliance Using Robot Skin," *IEEE Robotics and Automation Letters*, vol. 4, no. 4, pp. 4418–4423, 2019.
- [15] L. Rustler, M. Misar, and M. Hoffmann, "Adaptive electronic skin sensitivity for safe human-robot interaction," in *IEEE-RAS International Conference on Humanoid Robots (Humanoids)*. IEEE, 2024. [Online]. Available: <https://arxiv.org/abs/2409.06369>
- [16] R. J. Kirschner, N. Mansfeld, G. G. Peña, S. Abdolshah, and S. Haddadin, "Notion on the Correct Use of the Robot Effective Mass in the Safety Context and Comments on ISO/TS 15066," in *2021 IEEE International Conference on Intelligence and Safety for Robotics (ISR)*, 2021, pp. 6–9.
- [17] J. Rozlivek, A. Roncone, U. Pattacini, and M. Hoffmann, "Harmonious–human-like reactive motion control and multimodal perception for humanoid robots," *IEEE Transactions on Robotics*, 2024. [Online]. Available: <https://arxiv.org/abs/2312.02711>